Article

Developmental Cell

Fatty Acid Trafficking in Starved Cells: Regulation by Lipid Droplet Lipolysis, Autophagy, and Mitochondrial Fusion Dynamics

Graphical Abstract

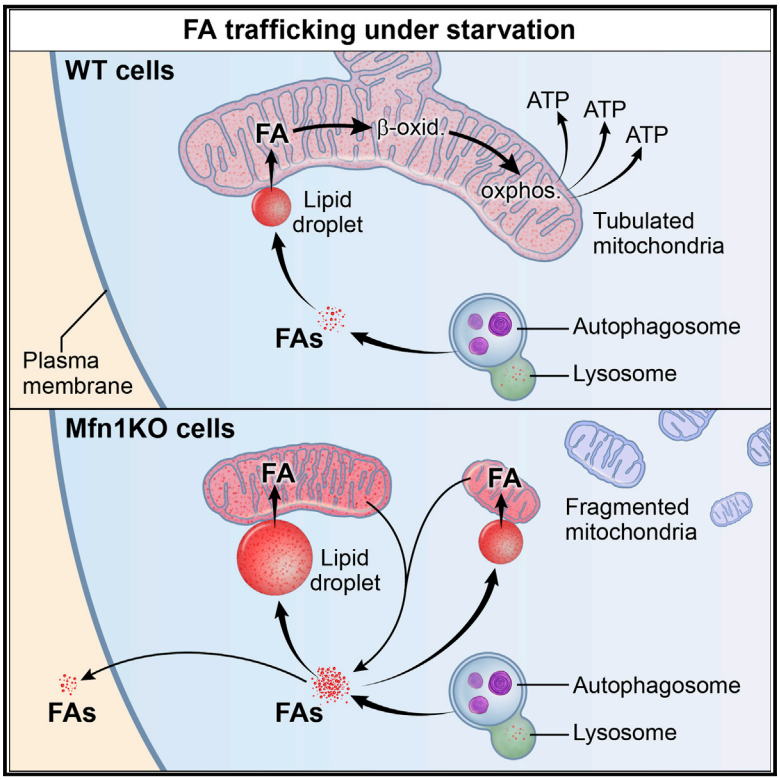

Highlights

- Starvation-induced autophagy supplies lipid droplets (LDs) with fatty acids (FAs)
- Cytoplasmic lipases release FAs from LDs for transfer into mitochondria
- Mitochondrial fusion is required to distribute and oxidize transferred FAs
- Mitochondrial fusion deficiency reroutes fatty acids to LDs and out of the cell

Authors

Angelika S. Rambold, Sarah Cohen, Jennifer Lippincott-Schwartz

Correspondence

lippincj@mail.nih.gov

In Brief

Mobilization of fatty acids (FAs) to mitochondria is crucial for cellular survival during nutrient stress. By visualizing FAs in live cells, Rambold et al. demonstrate that coordinated organelle dynamics—involving liberation of FAs from lipid droplets, autophagy, and mitochondrial fission/fusion—control FA flow to sustain mitochondrial respiration during nutrient stress.

Rambold et al., 2015, Developmental Cell *32*, 678–692
March 23, 2015
http://dx.doi.org/10.1016/j.devcel.2015.01.029

CellPress

Developmental Cell
Article

Fatty Acid Trafficking in Starved Cells: Regulation by Lipid Droplet Lipolysis, Autophagy, and Mitochondrial Fusion Dynamics

Angelika S. Rambold,[1,2,3] Sarah Cohen,[1,2] and Jennifer Lippincott-Schwartz[1,*]
[1]The Eunice Kennedy Shriver National Institute of Child Health and Human Development, NIH, Bethesda, MD 20892, USA
[2]Co-first author
[3]Present address: Max-Planck-Institute for Immunobiology and Epigenetics, Stübeweg 51, 79104 Freiburg, Germany
*Correspondence: lippincj@mail.nih.gov
http://dx.doi.org/10.1016/j.devcel.2015.01.029

SUMMARY

Fatty acids (FAs) provide cellular energy under starvation, yet how they mobilize and move into mitochondria in starved cells, driving oxidative respiration, is unclear. Here, we clarify this process by visualizing FA trafficking with a fluorescent FA probe. The labeled FA accumulated in lipid droplets (LDs) in well-fed cells but moved from LDs into mitochondria when cells were starved. Autophagy in starved cells replenished LDs with FAs, increasing LD number over time. Cytoplasmic lipases removed FAs from LDs, enabling their transfer into mitochondria. This required mitochondria to be highly fused and localized near LDs. When mitochondrial fusion was prevented in starved cells, FAs neither homogeneously distributed within mitochondria nor became efficiently metabolized. Instead, FAs reassociated with LDs and fluxed into neighboring cells. Thus, FAs engage in complex trafficking itineraries regulated by cytoplasmic lipases, autophagy, and mitochondrial fusion dynamics, ensuring maximum oxidative metabolism and avoidance of FA toxicity in starved cells.

INTRODUCTION

Cells adapt to nutrient starvation by shifting their metabolism from reliance on glucose metabolism to dependence on mitochondrial fatty acid (FA) oxidation. The biochemical basis for this metabolic reprogramming under starvation is well established (Eaton, 2002; Finn and Dice, 2006; Kerner and Hoppel, 2000; O'Neill et al., 2013). However, how FAs become mobilized and delivered into mitochondria for driving FA oxidation under starvation is far from clear.

FAs are stored within cells as energy-rich triacylglycerols in lipid droplets (LDs) in addition to being found on cellular membranes. Excess free FAs in the cytoplasm are harmful to cells: they can generate damaging bioactive lipids or disrupt mitochondrial membrane integrity (Unger et al., 2010). When mobilizing FAs from stores under starvation conditions, therefore, cells need to adjust FA trafficking pathways to avoid FA toxicity caused by overabundance of free FAs in the cytoplasm or within mitochondria.

Cells use two primary mechanisms for mobilizing FAs during nutrient stress. One is through autophagic digestion of membrane-bound organelles (i.e., the ER) or LDs (Axe et al., 2008; Hayashi-Nishino et al., 2009; Kristensen et al., 2008; Singh et al., 2009a; Ylä-Anttila et al., 2009). This involves autophagosomal engulfment of the organelle/LD and fusion with the lysosome, where hydrolytic enzymes digest the organelle/LD, releasing free FAs that quickly move into the cytoplasm (Singh et al., 2009a). When LDs are the substrate, this process is called lipophagy. While effective for bulk release of FAs into the cytoplasm in starved cells, FA mobilization by autophagy requires ways to avoid FA toxicity because of its potential to cause overabundance of free FAs in the cytoplasm. This could entail FAs either being immediately taken up into mitochondria or first moved to some storage compartment. Clearly, other FA trafficking pathways must function in conjunction with autophagy to manage released FAs in this mode of FA mobilization.

The second mechanism for mobilizing FAs during starvation is by lipolytic consumption of LDs. Here, cytoplasmic neutral lipases directly hydrolyze triacylglycerols on the LD surface. An advantage of this mechanism is that it can be regulated at the level of lipase activity, fine-tuned by the cell (Wang et al., 2008; Zechner et al., 2012). However, the fate of FAs released by this mechanism remains an issue. Do the FAs move directly from LDs into mitochondria (which is possible if LDs and mitochondria are in close proximity), or do the FAs first mix with cytoplasmic pools? If the former is true, how do cells ensure that all mitochondria obtain adequate levels of FAs to drive β-oxidation-based metabolism? If the latter is true, how do cells avoid FA toxicity? Given these unanswered questions, it is not surprising that the respective roles of autophagy and lipolysis (i.e., lipase digestion of LDs) in mobilizing FAs are ambiguous (Kim et al., 2013; Smirnova et al., 2006; Wang et al., 2008).

Mitochondria represent the primary site for β-oxidation where FAs are enzymatically broken down to sustain cellular energy levels during nutrient stress. This requires mitochondria to import FAs to yield the metabolic intermediates driving respiration (Eaton, 2002; Kerner and Hoppel, 2000; O'Neill et al., 2013). Upon starvation, cells upregulate enzymes required for mitochondrial FA import and β-oxidation (Eaton, 2002; Kerner and Hoppel, 2000). It is interesting that cells also remodel mitochondria into

highly connected networks (Gomes et al., 2011; Rambold et al., 2011) by modulating mitochondrial fission/fusion dynamics, regulated by proteins including fusion proteins, mitofusins 1 and 2 (Mfn1 and Mfn2) (on the outer mitochondrial membrane), optic atrophy protein 1 (Opa1) (on the inner mitochondrial membrane), and the fission protein dynamin-related protein 1 (Drp1) (Hoppins et al., 2007; Hoppins and Nunnari, 2009). It remains to be tested, however, whether mitochondrial fusion occurring during starvation facilitates FA trafficking and oxidation during nutrient stress.

Here, we investigate how cells coordinate FA mobilization, trafficking, and mitochondrial β-oxidation. Using a pulse-chase labeling method to visualize movement of FAs in live cells, we demonstrate that starved cells use primarily LDs as a conduit for supplying mitochondria with FAs for β-oxidation. This involves cytoplasmic, neutral lipase-mediated FA mobilization rather than lipophagy. Autophagy promoted lipid buildup in LDs, replenishing LDs with new FAs that then fluxed into mitochondria. Surprisingly, FA flux into mitochondria required LDs to be in close proximity with mitochondria and mitochondria to be highly tubulated/fused. This enabled FAs to distribute homogeneously inside mitochondria after import from LDs, ensuring FA oxidation, and downstream oxidative phosphorylation reactions were optimized. Defects in mitochondrial fusion caused massive alterations in cellular FA routing. Not only were nonmetabolized FAs redirected to and stored in LDs, but they also became excessively expulsed from cells. Given the role of FAs as signaling molecules, FA rerouting under these conditions could alter the function of entire cell populations, relevant to studies on obesity, diabetes, and mitochondrial disorders.

RESULTS

Nutrient Stress Increases FA Transfer from LDs to Mitochondria

Under starvation, cells shift to mitochondrial FA-driven oxidative phosphorylation for ATP production. This requires the transfer of FAs, including those stored in LDs, into mitochondria (Finn and Dice, 2006; Kerner and Hoppel, 2000). To understand how this process is regulated, we developed a pulse-chase assay to track FAs in relation to LDs and mitochondria in starved mouse embryonic fibroblasts (MEFs) (Figure 1A). For this assay, we utilized BODIPY 558/568 C_{12} (Red C12), a saturated FA analog with a tail composed of 12 carbons and a BODIPY 558/568 fluorophore covalently bound at the hydrophobic end, with an overall length approximately equivalent to that of an 18-carbon FA. BODIPY FAs have been used in studies of lipid trafficking and have been shown to incorporate into LD-specific neutral lipids (Herms et al., 2013; Kassan et al., 2013; Thumser and Storch, 2007; Wang et al., 2010). In our pulse-chase assay, cells were first labeled overnight with trace amounts (1 μM) of Red C12, which accumulated in neutral lipids within LDs (Figure 1B, 0h). They were then placed in complete or nutrient-depleted medium in the absence of Red C12 for 6 hr or 24 hr before labeling LDs or mitochondria and visualizing fluorescence in the cells with spinning-disk confocal microscopy.

Cells chased in nutrient-rich medium (i.e., complete medium, CM) showed nearly all Red C12 signal localized to LDs throughout the pulse-chase labeling period (Figure 1B, CM). Little, if any, Red C12 signal was transported into mitochondria (Figure 1C, CM). By contrast, cells in nutrient-depleted medium (i.e., Hank's balanced salt solution, HBSS) showed a dramatic loss of Red C12 signal from LDs between 6 and 24 hr of chase (Figure 1B, HBSS), with the signal redistributing into mitochondria (Figure 1C, HBSS). LD-to-mitochondria transfer of FAs in starved cells was already detectable within 6 hr (Figure 1C, HBSS; Figures S2A and S2B) and was most prominent after 24 hr (Figures 1C and 1D), with overall reduction of cellular Red C12 levels (Figure S1A). Near-complete overlap of Red C12 with MitoTracker-positive structures occurred after 24 hr of starvation, with no apparent labeling of other organelles (Figure 1C, HBSS).

Thin-layer chromatography (TLC) revealed that the amount of esterified Red C12 in cells decreased with time after nutrient deprivation, while the amount of free Red C12 increased (Figure 1E), consistent with our imaging results mentioned earlier. In addition, we observed slower migrating breakdown products of Red C12 with time after starvation. Inhibition of the mitochondrial FA importer CPT-I with etomoxir inhibited the translocation of Red C12 into mitochondria and the appearance of Red C12 breakdown products (Figures 1E, S1B, and S6E), indicating Red C12 as a substrate for β-oxidation. Thus, starvation initiates a process whereby cells selectively and efficiently transfer FAs from LDs to mitochondria for oxidation.

Cytoplasmic Lipase Activity Liberates FAs from LDs for Transfer to and Metabolism within Mitochondria

FAs can be released from LDs by two distinct mechanisms: lipolysis and lipophagy (Singh et al., 2009a; Zechner et al., 2012). To determine which of these two mechanisms is responsible for FA delivery to mitochondria under starvation, we used the Red C12 pulse-chase labeling protocol, examining the effect of inhibiting either lipase activity or autophagy.

To test the role of lipases in FA transfer to mitochondria, we depleted cells of adipose triglyceride lipase (ATGL) (Figure S2C), a ubiquitously expressed neutral lipase that can digest LDs (Smirnova et al., 2006), and then followed the fate of Red C12 during pulse-chase labeling. Unlike MEFs treated with noncoding control small interfering RNA (siRNA), which showed a dramatic increase in colocalization between Red C12 and MitoTracker after 24 hr starvation, ATGL-silenced MEFs showed only minimal redistribution of Red C12 from LDs into mitochondria (Figures 2A and 2B). Instead, the Red C12 signal remained localized to LDs (Figure 2A). Pharmacological inhibition of lipase function with diethylumbelliferyl phosphate (DEUP) also significantly reduced starvation-induced mitochondrial accumulation of Red C12 in the pulse-chase assay (Figures S2A and S2B, DEUP). Therefore, lipase activity is necessary for FA delivery from LDs into mitochondria in starved MEFs.

We next tested the role of autophagic activity in FA trafficking to mitochondria. Cells were pulse-chase labeled with Red C12 under starvation conditions in the presence of the autophagy inhibitor 3-methyladenine (3-MA). Notably, Red C12 trafficking into mitochondria was not significantly altered, compared to vehicle-treated cells (Figures S2A and S2B, 3-MA). To further test autophagy's role in FA delivery to mitochondria, we examined whether Red C12 transfer to mitochondria was affected in starved Atg5 knockout (Atg5KO) MEFs, in which autophagosome biogenesis is blocked (Mizushima et al., 2001). No

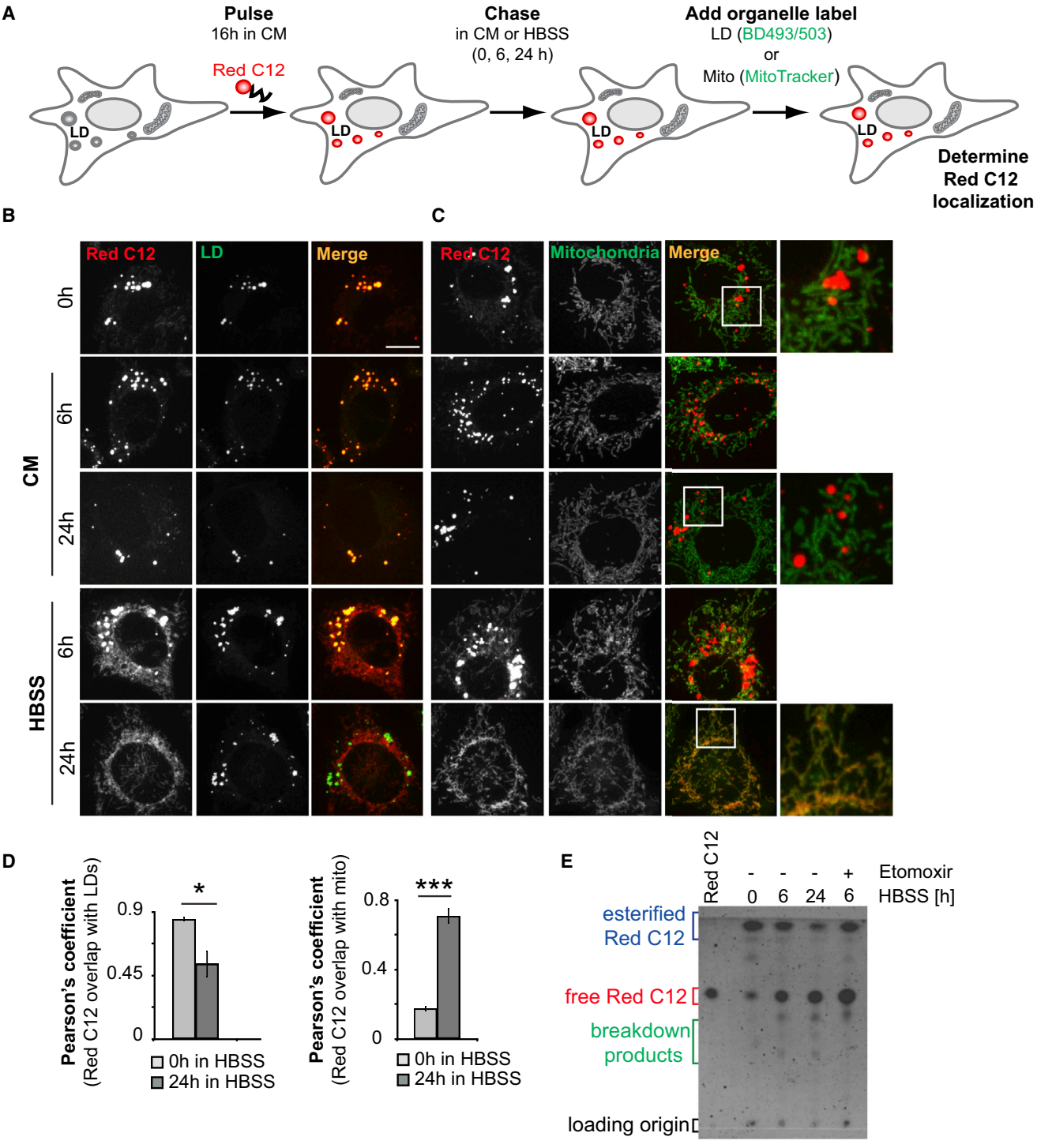

Figure 1. FA Trafficking Can Be Visualized using a Fluorescent FA Pulse-Chase Assay

(A) Schematic representation of the fluorescent FA pulse-chase assay: cells were pulsed with Red C12 overnight, washed, and incubated with CM for 1 hr in order to allow the Red C12 to accumulate in LDs. Cells were then chased in CM or HBSS for the indicated periods of time and imaged to determine the subcellular localization of the FA. h, hours; Mito, mitochondria.

(B–D) WT MEFs were assayed as described in (A) and chased in CM or HBSS for 0 hr, 6 hr, or 24 hr. (B) LDs were labeled using BODIPY 493/503, and (C) mitochondria were labeled using MitoTracker Green. Scale bar, 10 μm. (D) Relative cellular localization of Red C12 was quantified by Pearson's coefficient analysis. Data are expressed as means ± SEM. *$p < 0.05$; ***$p < 0.0001$.

(E) TLC resolving Red C12 isolated from WT MEFs assayed as described earlier and chased for 6 hr or 24 hr with HBSS in the absence or presence of etomoxir. See also Figure S1.

impairment in Red C12 transfer to mitochondria was observed (Figures 2C and 2D). TLC data corroborated the imaging results, with levels of esterified Red C12 decreasing in response to starvation in wild-type (WT) and Atg5KO, but not ATGL-depleted, MEFs (Figures 2G and 2H). It is interesting that, in ATGL-depleted MEFs, levels of free Red C12 still increased in response to starvation, indicating that compensatory mechanisms such as upregulation of phospholipase activity may exist (Cabodevilla et al., 2013).

The necessity of lipolysis (i.e., lipase digestion of LDs) for mitochondrial respiration under starvation was demonstrated by measuring mitochondrial oxygen consumption rate (mtOCR). Using DEUP treatment to inactivate lipases, we found that, in 6-hr-starved cells—but not fed cells—mtOCR levels were significantly reduced relative to those in untreated cells (Figure 2E; Figure S2G). By contrast, in similarly starved cells treated with 3-MA to inhibit autophagy, no reduction in mtOCR levels was observed (Figure 2F). However, autophagy inhibition at times of prolonged starvation significantly reduced mitochondrial respiration (Figure S2H), as reported previously (Singh et al., 2009a). Therefore, FA substrates used for mitochondrial respiration in acutely nutrient-stressed cells are primarily derived from lipolysis of LDs rather than through autophagy.

To address directly whether lipophagy is active in HBSS-starved MEFs, we performed colocalization studies between the autophagosomal marker LC3 and LDs. Although we detected lipophagy in individual MEFs (Figure S2E), autophagic LD degradation did not increase in 6-hr- or 24-hr-starved cells in HBSS relative to fed cells (Figures S2D–S2F). In contrast to HBSS, under milder starvation conditions, where only serum, but not amino acids and glucose, was limited, lipophagy was significantly induced (Figure S2E, 6h and 24h), as reported previously (Ouimet et al., 2011; Schulze et al., 2013; Singh et al., 2009a). Together, these data suggest that, under HBSS starvation conditions, MEFs are not reliant on lipophagy to supply mitochondria with LD-derived FAs. Rather, cytoplasmic neutral lipase activity, which releases FAs from LDs, appears to be the primary mechanism.

Autophagy Drives LD Growth during Starvation

Given that lipophagy is not induced in HBBS-starved MEFs, we next explored whether other autophagic pathways that are distinct from lipophagy play roles in regulating FA flux into mitochondria and sustaining mitochondrial metabolism in starved cells. Bulk autophagosomal degradation dramatically increases during starvation (Mizushima, 2007), so we investigated whether this type of autophagic activity helps recycle FAs to maintain LD stores for continual delivery of FAs to mitochondria. Supporting this possibility, we observed that BODIPY 493/503-labeled LDs grew continually in starved cells (Figure 3A), despite efficient transfer of pulsed Red C12 pools into mitochondria (Figure 1B). LD number almost doubled upon 6 hr of starvation and reached its maximum after 24 hr of starvation, with five times more LDs per cell (Figure 3B). The average LD size per cell increased by 2-fold after 24 hr of starvation (Figure 3B), shifting toward larger LDs in the heterogeneously sized LD population (Figure S3A). Finally, total LD volume per cell showed a significant increase (Figure S3B), and triglyceride storage, measured enzymatically, was boosted (Figure S3C).

As a further test of the hypothesis that autophagic activity during starvation helps maintain LD stores, we examined the effect of inhibiting autophagy on LD growth during starvation. No upregulation of LD abundance occurred in Atg5KO cells, compared to WT cells under starvation conditions (Figures 3C and 3D). LD number increase during starvation was also prevented by pharmacological inhibition of autophagy initiation using 3-MA (Figure S3D) or blocking lysosomal degradation of autophagosomes using bafilomycin A1 (Figure S3E).

To further confirm that autophagy-derived FAs drive LD growth in starved cells, we performed an FA pulse-chase assay using phosphatidylcholine that was fluorescent-tagged at its FA tail (FL HPC) (Figure 4A). Cells were first labeled overnight with trace amounts of FL HPC, which integrated into various cellular membranes, including the ER, mitochondria, and Golgi apparatus under fed conditions (Figure 4B, 0h CM; Figure S4A). Cells chased in CM retained the FL HPC signal in cellular membrane structures (Figure 4B, 6h CM). In contrast, in starved MEFs, the FL HPC signal on membranes was decreased due to its redistributing into LDs (Figure 4B, 6h HBSS; Figure S4B). Inhibition of autophagy using 3-MA, bafilomycin A1, or Atg5-deficient MEFs reduced this transfer (Figures 4B and 4C).

The active involvement of autophagy in FL HPC recycling from cellular membranes was further confirmed by colocalization studies in MEFs transfected with the autophagosomal marker mCherry-LC3 or lysosomal marker LAMP1-mCherry. Upon starvation, FL HPC could be partially found in autophagosomes/lysosomes (Figures 4D and 4E) in addition to LDs (Figure 4B). Autophagosome/lysosome localization could be prevented by 3-MA (Figures 4D and 4E, 3-MA). When autophagosome-lysosome fusion was reduced with high concentrations of bafilomycin A1 (Bjørkøy et al., 2005), significant trapping of FL HPC in autophagosomes occurred (Figures 4D and 4F). In addition, there was less localization of FL HPC with lysosomes labeled with LAMP1 (Figure 4E, BafA1) and with late endosomes labeled with Rab5 (Figure S4C). Together, these data suggest that autophagy is involved in shuttling FL HPC from cellular membranes into lysosomes. FAs hydrolyzed from the phospholipids would then be released into the cytoplasm and associate with LDs.

Fused Mitochondria Ensure that FAs Are Distributed throughout Mitochondria for Maximal β-Oxidation

When starved MEFs were imaged after expression of the mitochondrial marker mito-RFP (red fluorescent protein) and labeling with the LD marker BODIPY 493/503, we found that virtually all LDs were closely associated with mitochondria (Figure 5A). Monitoring mitochondria and the distribution of FAs delivered into them in starved cells further revealed that mitochondria were highly fused and that FAs were homogenously distributed throughout the mitochondria (Figures 5A and 5D) (Gomes et al., 2011; Rambold et al., 2011). One interpretation of these results is that close association between LDs and mitochondria allows FAs to traffic directly from LDs into mitochondria. The fused state of mitochondria, in turn, would ensure that FAs are equilibrated throughout the mitochondrial system (assuming limited numbers of LDs per cell), maximizing FA availability for β-oxidation reactions.

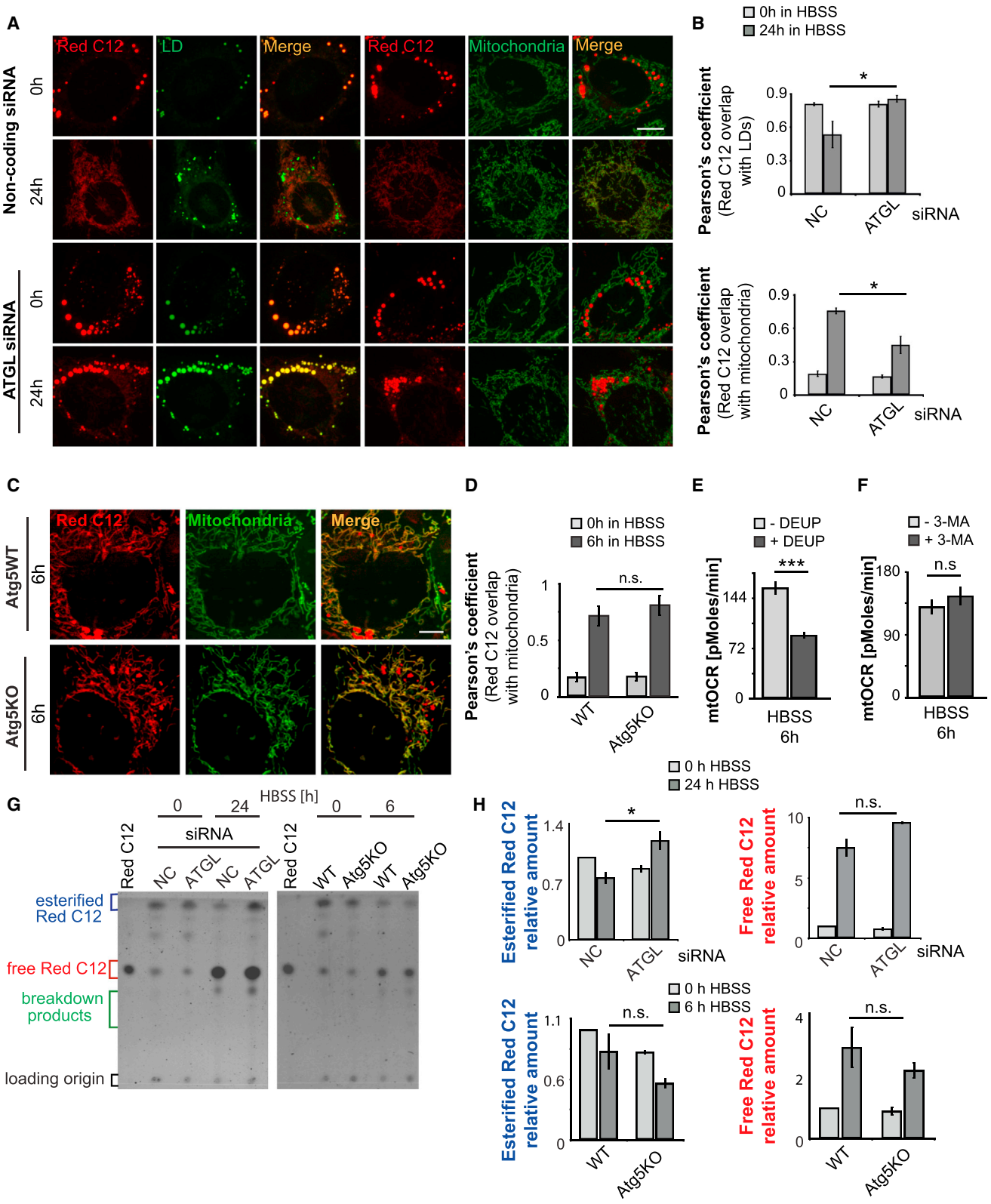

Figure 2. Cytoplasmic Lipase Activity, but Not Lipophagy, Is Essential to Liberate FAs from LDs for Transfer to Mitochondria

(A) WT MEFs were assayed as described in Figure 1A after RNAi using noncoding or ATGL siRNA. Scale bar, 10 μm. h, hours.

(B) Quantification of the correlation between Red C12 signal and LDs (upper graph) or mitochondria (lower graph) in the experiment shown in (A). NC, noncoding.

(C) Atg5-WT and Atg5-deficient cells were assayed as described in Figure 1A. Scale bar, 10 μm.

(legend continued on next page)

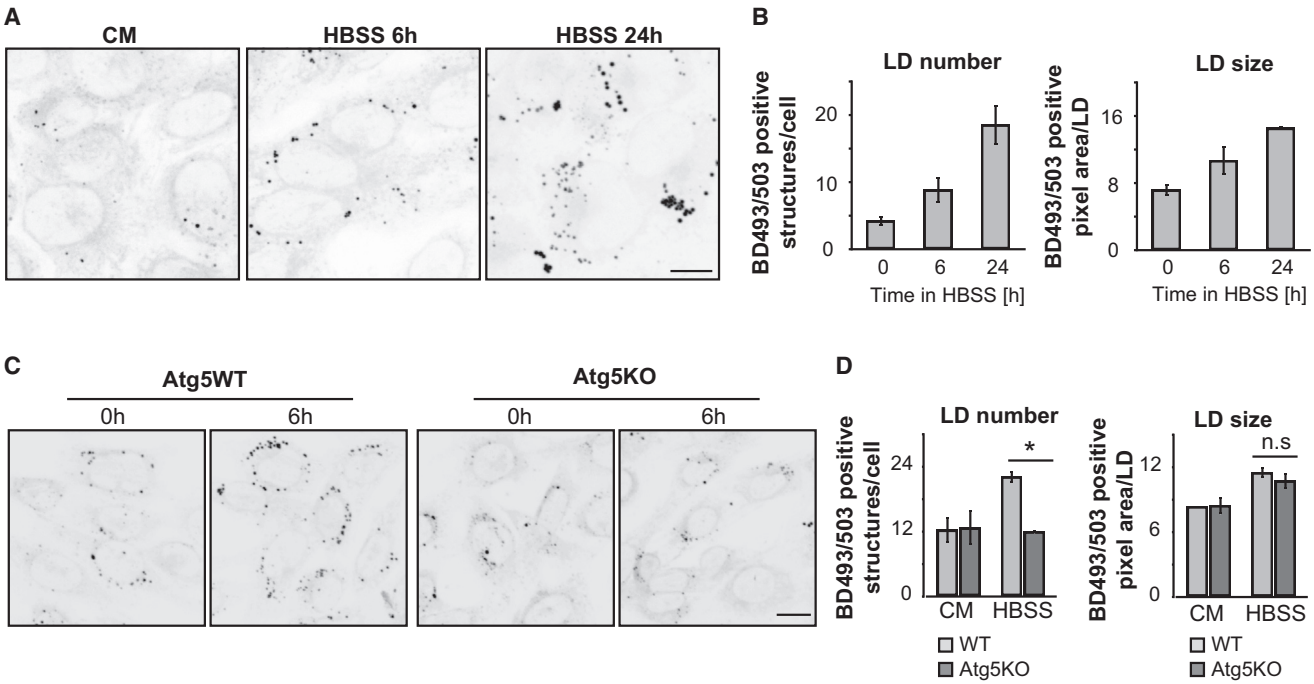

Figure 3. Autophagy Drives LD Growth during Starvation

(A–D) WT or Atg5KO MEFs were incubated in CM or HBSS for the time periods indicated, BODIPY 493/503 was added to visualize LDs, and images of live cells were captured and presented as inverted grayscale micrographs (A and C). To determine LD growth during starvation LD size and number were measured (B and D). Scale bars, 50 μm. Data are expressed as means ± SEM. *p < 0.05; n.s., not significant.

See also Figure S3.

To test this hypothesis, we first examined whether the fused state of mitochondria was necessary for the homogenous dissemination of FAs within mitochondria. Red C12 pulse-chase labeling was performed in MEFs deficient in the major mitochondrial fusion proteins Mfn1 or Opa1. In the Mfn1 knockout (MfnKO) or Opa1 knockout (Opa1KO) cells, mitochondria did not form networks and were fragmented (Figure 5A) (Chen et al., 2005; Gomes et al., 2011; Rambold et al., 2011). Despite this, LDs were still in close proximity with mitochondria, and there was transfer of Red C12 into mitochondrial elements (Figures 5A, 5B, and 5D). However, many mitochondrial elements were not in close proximity to LDs (Figure 5C), and Red C12 did not become homogenously distributed across the mitochondrial population (Figure 5D), resulting in either very low or exceedingly high Red C12 signals relative to those detected in WT cells (Figure 5D). In contrast to Red C12, MitoTracker signal was uniform throughout the mitochondria of WT, Mfn1KO, and Opa1KO cells (data not shown). Therefore, mitochondrial fusion is required to homogenously distribute LD-derived FAs throughout the mitochondrial network in starved cells.

We next investigated whether a homogenous distribution of FAs throughout mitochondria is necessary for optimal β-oxidation within mitochondria in starved cells. To address this, we measured FA-driven mtOCR and its contribution to total mtOCR in control or Mfn1KO cells under starvation. Mfn1KO cells were used as a primary model since, unlike Opa1KO and Mfn1/2KO MEFs (Chen et al., 2005; Cogliati et al., 2013; Frezza et al., 2006) (Figure S5A), their respiration levels under fed conditions (Figures 5E and 5F) and mitophagy levels under starvation conditions (Figure S5B) were comparable to those of WT cells. In starved WT cells, there was an expected rapid increase in FA oxidation over 6 hr, followed by sustained oxidation for at least 24 hr (Figures 5E and 5G). The boosted β-oxidation enabled these cells to nearly maintain equivalent total mitochondrial respiration levels over the entire starvation period (Figures 5F and 5H). Mfn1-deficient cells upregulated initial levels of β-oxidation comparable to control cells; however, the levels were not maintained over 24 hr, with FA oxidation becoming significantly reduced (Figures 5E and 5G). Consequently, total mitochondrial respiration levels in Mfn1KO cells dropped

(D) Quantification of the correlation between Red C12 signal and mitochondria in the experiment described in (C).

(E and F) Mitochondrial respiration is dependent on cytoplasmic lipase activity. Mitochondrial respiratory activity of 6-hr-starved WT MEFs was measured in the presence of (E) the lipase inhibitor DEUP and (F) 3-MA to inhibit autophagy.

(G) TLC resolving Red C12 isolated from cells assayed as described in (A) (left panel) or (C) (right panel).

(H) Relative amounts of esterified and free Red C12 were quantified from images of TLC plates, normalized to Red C12 levels of WT cells at the 0-hr time point. Data are expressed as means ± SEM. *p < 0.05; ***p < 0.0001; n.s., not significant. See also Figure S2.

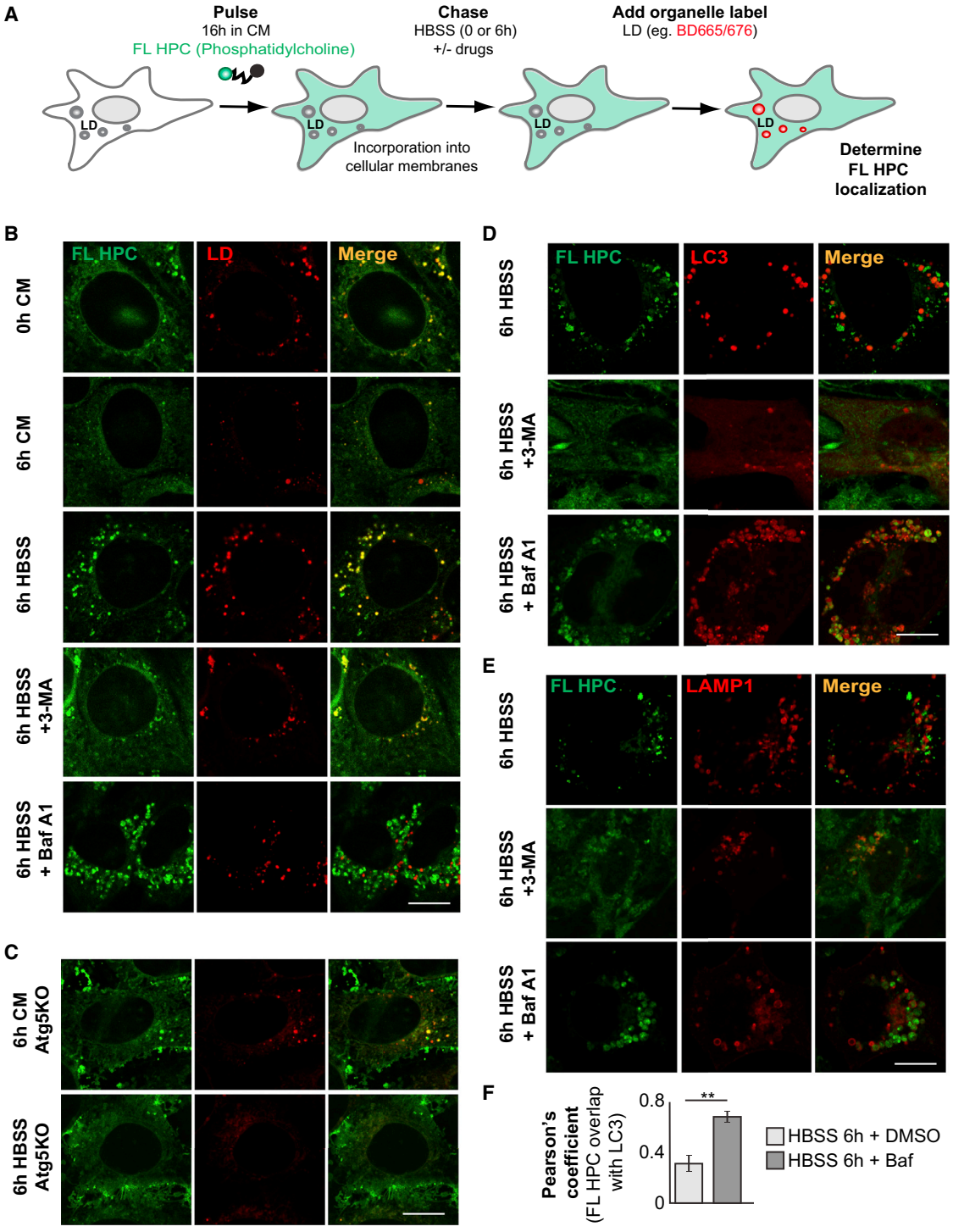

Figure 4. Autophagy Mobilizes Phospholipids from Cellular Membranes during Starvation

(A and B) FL-HPC-loaded WT MEFs were chased in HBSS for 6 hr in the absence or presence of 3-MA or bafilomycin A1 (Baf A1), and the subcellular localization of FL HPC was determined. LDs were stained with BODIPY665/676. h, hours.

(C) Atg5KO MEFs were assayed as described in Figure 4A.

(D and E) WT MEFs expressing mCherry-LC3 or LAMP1-mCherry were assayed as described in Figure 2A.

(F) Quantification of the correlation between FL HPC signal and autophagosomes in the experiment described in Figure 2D. Data are expressed as means ± SEM. **$p < 0.001$.

Scale bars, 10 μm. See also Figure S4.

significantly over time (Figure 5H), accompanied by excessive accumulation of mitochondrial FA breakdown intermediates (Figure S6E).

We next determined whether the requirement of having fused mitochondria was specific for FA metabolism and not for metabolism of other metabolic substrates, such as glutamine. Unlike FAs, which are concentrated in LDs, glutamine is diffusely distributed in the cytoplasm and is taken up into mitochondria via transporters distributed throughout the organelle. The fused state of mitochondria may, therefore, be irrelevant for glutamine to be effectively metabolized. To address this possibility, we measured mtOCR levels in starved cells cultured for 24 hr with and without glutamine addition in WT and Mfn1KO cells. A 1.3-fold induction of mitochondrial respiration in response to glutamine addition occurred for both control and Mfn1KO cells (Figure 5I). This revealed that mitochondrial fragmentation does not affect glutamine oxidation, unlike its effect on oxidation of FAs. Therefore, β-oxidation requires mitochondria to be highly fused, in contrast to other mitochondrial reactions such as glutamine oxidation, which are unaffected by mitochondrial morphology. This could be explained if delivery of FAs to mitochondria occurs primarily at limited sites (i.e., LDs in close proximity to mitochondria), thereby requiring the mitochondrial system to be highly fused to equilibrate newly arriving FAs.

Defects in Mitochondrial Fusion Lead to Lipid Accumulation in LDs

Previous work has shown that FA buildup can be toxic to mitochondria (Unger et al., 2010) and that cells from patients with inherited β-oxidation defects can re-export FAs out of mitochondria (Nada et al., 1995; Schaefer et al., 1995). Given the observed heterogeneous buildup of mitochondrial FAs in starved Mfn1KO or Opa1KO cells, we explored how mitochondria cope with an excessive load of nonmetabolized FAs. One possibility is that the cells redirect FAs back to LDs to be esterified to inert triacylglycerols. This predicts a buildup of LDs in these cells. Consistent with this, live-cell imaging of BODIPY 493/503 in Mfn1KO and Opa1KO cells in CM showed slightly higher cellular LD load than WT cells as measured by increased LD size, number, and volume (Figure 6A). The increase in LD number and size was more pronounced when mitochondrial-fusion-deficient cells were starved, with three times higher LD volume per cell occurring compared to that in fusion-competent control cells (Figures 6B and 6C). Pulse-chase Red C12 labeling experiments further revealed that, although net transfer of Red C12 into mitochondria in starved cells deficient in mitochondrial fusion was not significantly affected (Figures S6A and S6D), there was greater buildup of the Red C12 in LDs (Figures S6A–S6C). Greater accumulation of Red C12 in LDs was also seen in nonstarved cells deficient in mitochondrial fusion compared to WT cells, with Opa1KO cells showing a more extreme phenotype than Mfn1KO cells, most likely because of their increased bioenergetic deficiency (Figures S6A–S6C). Despite this, lack of Mfn1 or Opa1 did not affect overall FA release from LDs or the abundance of the mitochondrial FA importer CPT-I under starvation conditions (Figures S6C and S6F). Together, these results suggest that, to compensate for their inability to effectively metabolize FAs, mitochondrial fusion-deficient cells reroute FAs to reassociate with LDs.

Defects in Mitochondrial Fusion Lead to Increased FA Expulsion from Cells

Given that LD storage capacity is thought to be limited in cells of nonadipose origin, we wondered if cells deficient in mitochondrial fusion used further coping mechanisms to limit free FA levels in their cytoplasm. One mechanism would be to transfer FAs into the extracellular space (Herms et al., 2013). To test this possibility, we combined Red C12 labeling of FAs with a cellular coculture system to serve as optical readout for FA release (Figure 7A). WT MEFs were pulsed with Red C12, and the resulting "donor" cells were then cocultured for 24 hr in nutrient-depleted medium with "acceptor" WT MEFs labeled with a green cellular dye. A small amount of Red C12 was transferred from WT donor cells to acceptor cells (Figures 7B and 7C). These results demonstrate that FAs are exported at low levels in MEFs during starvation. Inhibiting FA release from LDs by ATGL depletion drastically reduced FA transfer into acceptor cells (Figure S7A), thus verifying LD stores as a major source for the FA expulsion. Performing coculture experiments with Mfn1KO donor cells revealed both higher levels of donor cell labeling and significant transfer of Red C12 into the WT acceptor cells, as shown both by fluorescence imaging and quantitative flow cytometry (Figures 7B and 7C). Similar high levels of starvation-induced Red C12 release were also observed in fusion-deficient Opa1KO cells (Figures 7B and 7C). Since cell survival rates in Mfn1KO and Opa1KO cells were comparable to those in WT cells (Figure S7B), we can exclude the possibility that transferred FAs were released from dying cells. Together, these data suggest that reduction in β-oxidation rates, induced by mitochondria fusion deficiency, increases rates of FA efflux out of cells. This could be an important compensatory mechanism to avoid toxic FA buildup in the cytoplasm.

DISCUSSION

In this study, we define the pathways regulating FA flux into mitochondria during nutrient stress, crucial for enabling cells to shift their metabolism to FA oxidation and, thereby, survive starvation. Using pulse-chase labeling assays, we found that FA flux into mitochondria was codependent on LD lipolysis, autophagy, and mitochondrial fusion dynamics (Figure 7D). Unless all three systems contributed, FAs did not successfully redistribute into and throughout mitochondria to maximize oxidative phosphorylation and, instead, accumulated within LDs and/or were released from cells. As discussed in the following text, our findings are relevant to the broader question of how cells and organisms adapt cellular FA flow and storage to changing nutrient availability and metabolic need.

In exploring how FAs move into mitochondria in starved cells, we found that rather than being delivered from a free cytoplasmic pool (as occurs for other metabolites), FAs used LDs as their conduit. This may explain why LDs and mitochondria are so closely associated; it would enable FAs to move efficiently between these two organelles. Close spatial positioning of LDs and mitochondria has been reported before in various cell types (Shaw et al., 2008; Sturmey et al., 2006; Tarnopolsky et al., 2007; Vock et al., 1996). Indeed, electron microscopic studies of skeletal muscle showed chains of alternating mitochondria-LD structures (Tarnopolsky et al., 2007), with

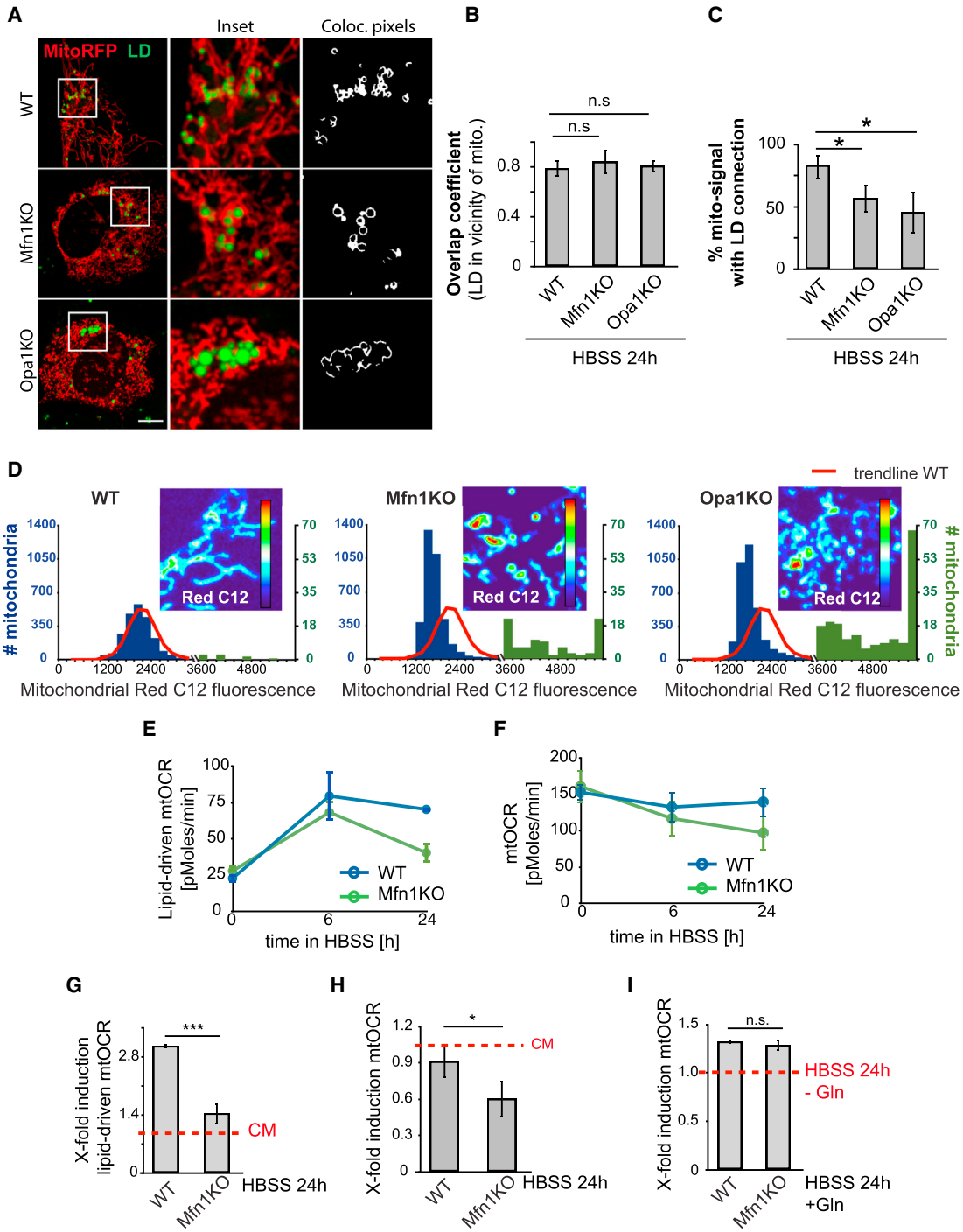

Figure 5. Mitochondrial Fusion Is Required for Mitochondrial FA Distribution and Oxidation

(A–C) WT, Mfn1KO, or Opa1KO MEFs were transfected with the mitochondrial marker mito-RFP and labeled with BODIPY 493/503 to visualize LDs. (A) Live images were acquired, (B) the ability of LDs to gain states of high proximity to mitochondria (mito.) was measured using the overlap coefficient, and (C) overall mitochondrial content with direct contact to LDs was measured. h, hours; Coloc., colocalized.

(D) Red C12 localization in WT, Mfn1KO, or Opa1KO MEFs was assayed as described in Figure 1A (24 hr HBSS). Red C12 intensities in individual mitochondria were plotted as histograms, with blue and green bars representing higher and lower ranges of intensities, respectively. Red lines: WT trendline. Representative images of mitochondrial Red C12 in each cell line were presented as heatmaps: blue indicates lowest and red indicates highest mitochondrial Red C12 levels.

(E and F) Mitochondrial respiratory activity was measured in WT and Mfn1KO MEFs, incubated in CM or HBSS for the time points indicated. (E) Lipid-driven mtOCR and (F) total mtOCR were determined. Lipid-specific respiration was analyzed by acute CPT-I inhibition with etomoxir.

(legend continued on next page)

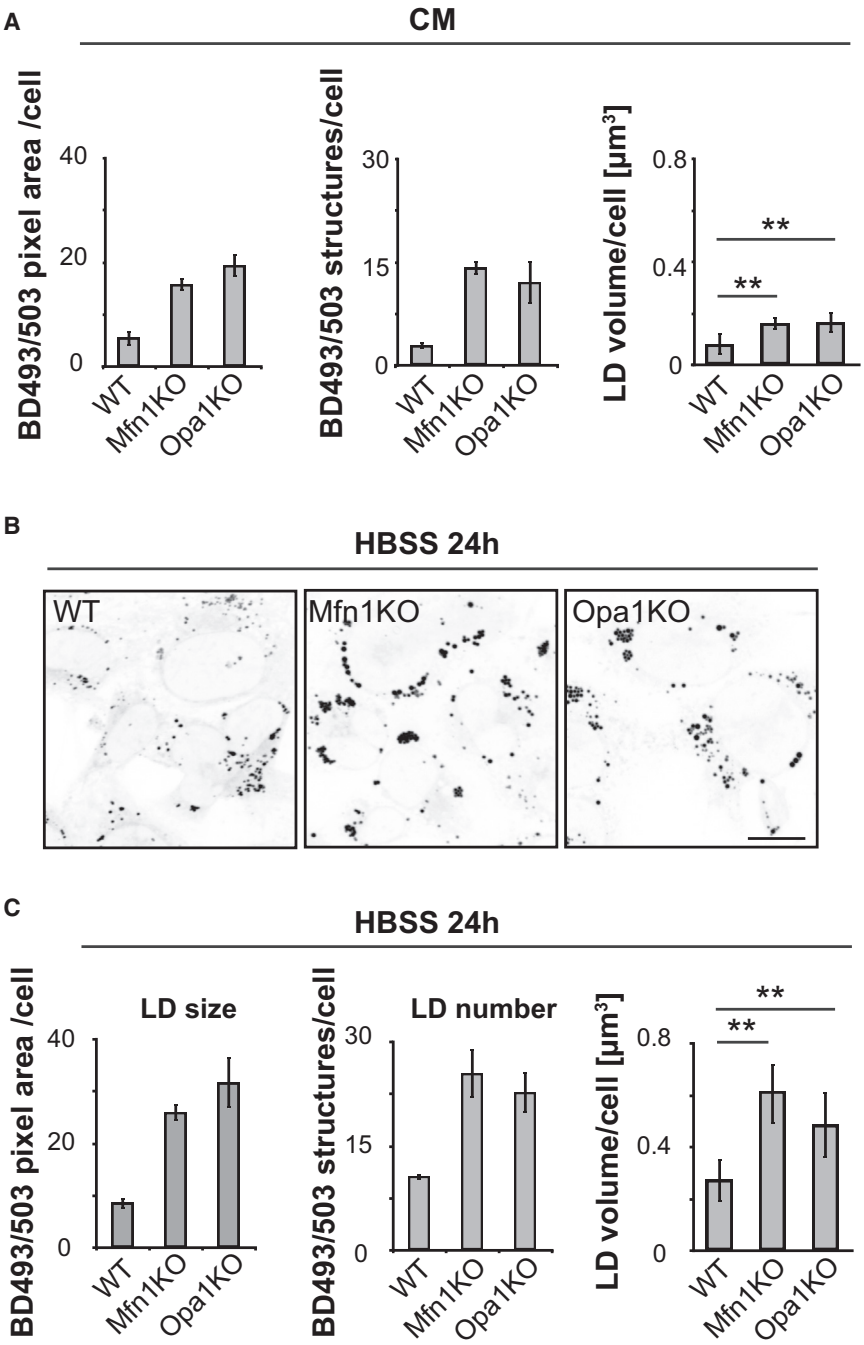

Figure 6. Mitochondrial Fusion Deficiencies Result in Increased FA Storage

(A–C) WT, Mfn1KO, and Opa1KO cells were grown in (A) complete or (B and C) starvation medium for 24 hr, BODIPY 493/503 was added to visualize LDs, and LD size, number, and volume were determined.

Scale bar, 50 μm. Data are expressed as means ± SEM. **p < 0.001. See also Figure S6.

FA release from LDs has been linked to cytoplasmic lipases and lipophagy (i.e., autophagic digestion of LDs), with their relative contributions still unclear. Recent studies identified pleiotropic roles for autophagy in lipid metabolism that may be tissue or condition specific (Dupont et al., 2014; Kim et al., 2013; Shibata et al., 2009, 2010; Singh et al., 2009a, 2009b). Here, we demonstrated that, during acute starvation in mammalian cells, autophagy is dispensable for supplying mitochondria with FAs to sustain oxidative respiration. This is because inhibiting lipase activity (by silencing ATGL or treating with DEUP), which blocked FA flux into mitochondria, reduced mitochondrial oxidative metabolism and resulted in enlarged LDs in starved cells. By contrast, we found that conditions of serum depletion in the presence of amino acids and glucose led to upregulation of lipophagy, consistent with previous studies (Ouimet et al., 2011; Schulze et al., 2013; Singh et al., 2009a). How the availability of different nutrients dictates autophagosomal specificity remains to be addressed. One possibility is that the signaling pathways that control autophagy are sensitive to different nutrient stress, and this determines what substrate is targeted. For example, the major autophagy regulator mammalian target of rapamycin (mTOR) is rapidly inactivated during HBSS starvation but not during serum starvation alone (Peterson et al., 2011). Additionally, specialized cell types might differentially utilize lipases versus lipophagy for their response to starvation; for example, release of FAs from LDs by autophagy might be of particular importance in cell types with low lipase activity, such as hepatocytes (Singh et al., 2009a; Walther and Farese, 2012).

increased interactions in response to energy-intensive exercise (Shaw et al., 2008). It remains to be established what mechanisms underlie the close positioning of LDs and mitochondria, but roles for microtubules (Valetti et al., 1999; Welte et al., 2005), SNAP23 (Jägerström et al., 2009), and perilipin 5 (Wang et al., 2011) have been proposed.

(G and H) Respiratory induction levels for lipid-driven mtOCR and total mtOCR levels were determined, using mtOCR levels in CM as baseline levels for each cell line.

(I) Glutamine (Gln)-driven respiration was determined by acute injection of glutamine to 24-hr-starved cells, and induction levels were determined.

Scale bar, 10 μm. Data are expressed as means ± SEM. *p < 0.05; ***p < 0.0001; n.s., not significant. See also Figure S5.

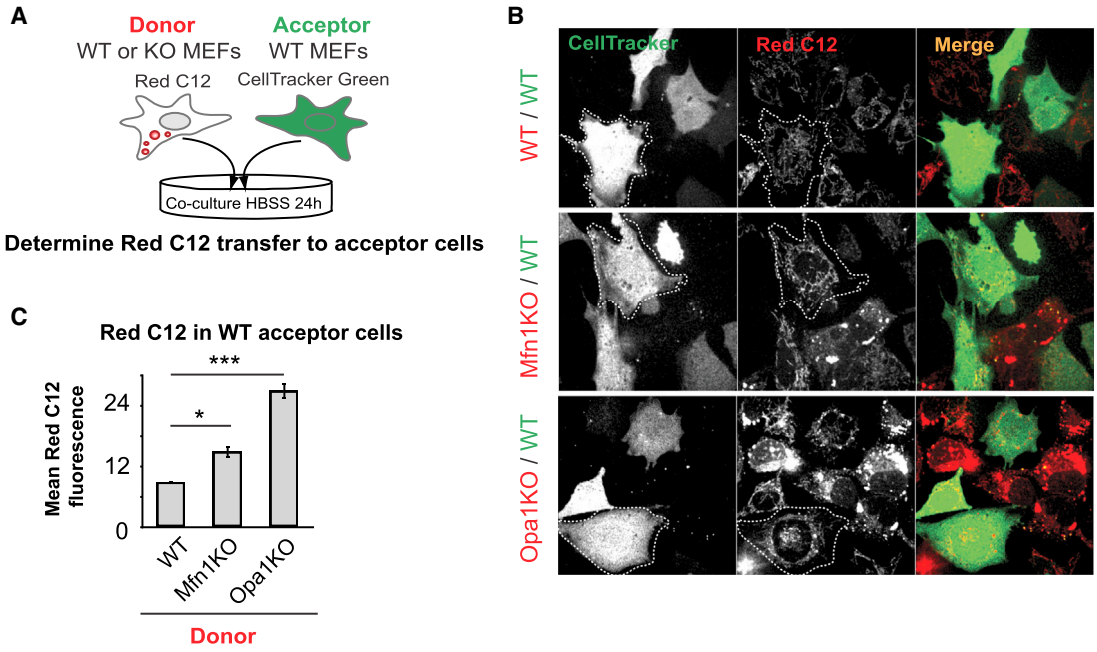

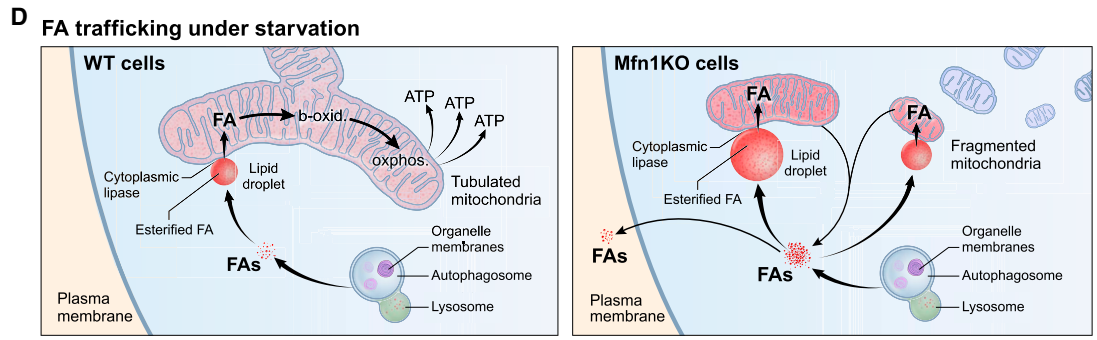

Figure 7. Mitochondrial Fusion Deficiencies Result in Increased Cellular Export of FAs

(A) Schematic representation of the coculture assay to visualize cellular FA export. Red C12 prelabeled donor cells (WT, Mfn1KO, or Opa1KO MEFs) were washed excessively and then cocultured for 24 hr in HBSS with CellTracker-green-labeled acceptor cells (WT MEFs).

(B and C) In (B), live cell images of donor and acceptor cells were acquired, and (C) levels of Red C12 transfer into acceptor cells measured by flow cytometry analysis. Data are expressed as means ± SEM. *$p < 0.05$; ***$p < 0.0001$.

(D) Model of FA trafficking in starved cells. In WT cells, autophagy releases FAs from phospholipids within organelle membranes; these FAs flux through LDs into tubulated mitochondria, where they become homogenously distributed throughout the mitochondrial network and are efficiently metabolized to produce ATP. In fusion-deficient Mfn1KO cells, fragmented mitochondria receive highly variable amounts of FA. These FAs are not efficiently metabolized, leading to redirection of FA flow, which results in increased FA storage within LDs and efflux of FAs from the cell. b-oxid., β-oxidation; oxphos, oxidative phosphorylation.

See also Figure S7.

Why do starved mammalian cells prefer lipolysis to lipophagy in trafficking FAs into mitochondria? We speculate that this arises from several factors. One factor relates to avoidance of FA overload and toxicity. When FA levels become too high in the cytoplasm, FA toxicity occurs, leading to membrane permeability and mitochondrial dysfunction (Unger et al., 2010). Digestion of LDs by autophagy would likely release the stored FAs in large quantities from lysosomes into the cytoplasm, requiring coordination of FA flux into mitochondria with storage of excess FAs in LDs. By contrast, FA flux into mitochondria via lipolysis would only require regulation of lipases and LD-associated proteins, such as perilipin 5 (Dalen et al., 2007; Granneman et al., 2011; Wolins et al., 2006; Yamaguchi et al., 2006). Close positioning of LDs with mitochondria, which we observed, could provide a further mechanism whereby high concentrations of FAs flow directly from LDs into mitochondria, avoiding buildup in the cytoplasm. This transfer of FAs is likely to occur in association with FA-binding proteins (FABPs), a family of small cytoplasmic proteins capable of reversibly binding FAs with high affinity. The ubiquitously expressed heart FABP (H-FABP), in particular, has been implicated in the transfer of FAs to mitochondria (Furuhashi and Hotamisligil, 2008). Once locally delivered into mitochondria, the FAs could then readily distribute throughout the mitochondrial system, given the highly fused

state of mitochondria in starved cells (Gomes et al., 2011; Rambold et al., 2011).

A second factor for why starved mammalian cells might prefer lipolysis to lipophagy for trafficking of FAs into mitochondria could be related to the FA species released by lipolysis versus lipophagy. The FA forms generated by lipolysis may be more readily imported into mitochondria (or metabolized there), compared to FAs released during lipophagy. In line with this, a recent report demonstrated that lipid-dependent peroxisome proliferator-activated receptor (PPAR) signaling specifically requires cytoplasmic lipase-catalyzed hydrolysis of intracellular triglyceride stores, but not FAs from other sources, to build a functional signaling complex (Haemmerle et al., 2011). Given that lipase-activated PPAR signaling drives mitochondrial biogenesis and oxidative phosphorylation, FA release from LDs could contribute to the coordination between FA transfer to mitochondria and regulation of mitochondrial activity. Finally, it is even conceivable that components of LDs, such as LD-associated proteins, dissociate during lipolysis and regulate FA trafficking or import.

Given that FAs flux into mitochondria from LDs via lipolysis in starved cells, what supplies LDs with FAs so they can be continuously delivered into mitochondria? We found that this function is mediated by autophagy. Autophagic digestion of cellular membranes released FAs into the cytoplasm from where they were at least partially incorporated into LDs. Therefore, inhibiting autophagy did not prevent FAs from moving into mitochondria and driving β-oxidation as long as LDs were abundant.

Notably, we found that effective FA delivery into mitochondria in starved cells involved a role for mitochondrial fusion dynamics. Unless mitochondria were highly fused, FAs did not distribute homogenously throughout the mitochondrial system, and energy production within mitochondria by oxidative phosphorylation was reduced. In cells with fragmented mitochondria, FAs excessively accumulated in some mitochondrial elements and diminished in others, presumably due to only some mitochondrial elements being associated close to a LD. The consequence of these effects on FA trafficking and metabolism were major, with levels of FA metabolism reduced, more FAs built up in LDs, and more FAs fluxed out of the cell to neighboring cells.

Changes in mitochondrial shape and ultrastructure are known to accompany lipid-associated diseases and cellular lipid excess (Galloway and Yoon, 2012, 2013; Yoon et al., 2011). Our results showing the functional interrelation of mitochondrial fusion with cellular FA trafficking inside and between cells provide conclusive evidence that alterations in mitochondrial structural integrity can actively contribute to changes in cellular lipid homeostasis. Our data are consistent with a model in which mitochondrial-fusion-deficient cells respond to reduced β-oxidation levels by rerouting FAs from mitochondria into LDs and the extracellular medium, similar to studies showing that mitochondrial import enzymes reverse FA transport when β-oxidation is impaired (Eaton et al., 1996; Nada et al., 1995; Schaefer et al., 1995; Watmough et al., 1988). The level of FA rerouting was dosage dependent, with higher FA flux occurring in respiratory defective Opa1KO than in Mfn1KO cells. The correlation between respiratory deficiency and FA export might make FA rerouting also relevant for metabolic defects resulting from mechanisms other than altered mitochondrial fission/fusion dynamics.

The system we have described for mobilizing FAs during starvation may play a role in other cellular contexts. For example, FA oxidation is critical in highly oxidative cells, like skeletal muscle specifically during exercise or the heart (Fritz et al., 1958; Grynberg and Demaison, 1996). Emerging evidence is also correlating the presence of fused mitochondria with many cellular states of high-energy demand, including G1/S cell-cycle transition (Mitra et al., 2009) and chemical stress (Tondera et al., 2009). Moreover, recent studies showed that fusion is required to sustain mitochondrial activity during excitation-contraction coupling in skeletal muscle and the activity of Agrp neurons in lipid-fed mice (Dietrich et al., 2013; Eisner et al., 2014). In addition, because FAs and their derivatives play important roles in regulating cellular signaling cascades and contribute to FA-driven modulations in metabolism, inflammatory responses, and cell death programs (Calder, 2013; Wahli and Michalik, 2012; Zechner et al., 2012), alterations in their levels likely have huge health risks (Currie et al., 2013; Krahmer et al., 2013). Therefore, future work studying the FA flux system described here (involving autophagosomes, LDs, and mitochondria) has great potential for contributing to our understanding of the pathophysiology of lipid-associated diseases, such as obesity, diabetes, cancer, and inflammatory disorders.

EXPERIMENTAL PROCEDURES

Fluorescent FA Pulse-Chase and Coculture Experiments

MEFs were incubated with CM (DMEM with 10% fetal bovine serum and 4 mM glutamine) containing 1 μM BODIPY 558/568 C_{12} (Red C12, Life Technologies) or 2 μM β-BODIPY FL C_{12}-HPC (FL HPC, Life Technologies) for 16 hr. Cells were then washed three times with CM, incubated for 1 hr in order to allow the fluorescent lipids to incorporate into LDs or cellular membranes, and then chased for the time indicated in CM or HBSS in the absence or presence of various drugs. Mitochondria were labeled with 100 nM MitoTracker Green FM (Life Technologies) for 30 min prior to imaging. To label LDs, BODIPY 493/503 (Life Technologies) or BODIPY 665/676 (Life Technologies) was added to cells at 200 ng/ml immediately prior to imaging and was present during imaging.

For FA transfer coculture assays, donor cells were incubated with 2 μM Red C12 for 16 hr in CM. Cells were then washed three times with CM followed by 1 hr incubation. In parallel, acceptor cells were labeled for 30 min at 37°C with 5 μM CellTracker Green (Life Technologies), according to the manufacturer's instructions. Acceptor cells were trypsinized and coplated with donor cells. After 24 hr in HBSS, either cells were imaged, or BODIPY 558/568 C_{12} fluorescence was determined in CellTracker-Green-positive acceptor cells using a FACSCalibur cell analyzer (BD Biosciences).

Image Processing, Analysis, and Statistics

Images were analyzed using Slidebook Imaging Software (3i) and ImageJ (NIH). Image brightness and contrast were adjusted in Adobe Photoshop CS.

For fluorescent FA pulse-chase assays, z stacks were analyzed using Slidebook to determine Pearson's coefficients and mean fluorescence intensity. To quantify the fluorescence intensity of Red C12 in mitochondria, we made a mask using the MitoTracker channel, and then the mean fluorescence intensity in the Red C12 channel was calculated either across the entire mask or for individual objects larger than ten pixels.

For LD-mitochondria proximity, binary z stack images were analyzed using ImageJ "JACoP" software to determine the overlap coefficient. For connectivity between mitochondria and LDs, a mask was created from segmented mitochondrial images, and the percentage of mitochondrial signal connected to a site of LD-mitochondria proximity versus total mitochondrial signal was calculated.

LD size and number were quantified with the ImageJ "analyze particles" function in thresholded images, with size (square pixel) settings from 0.1 to 100 and circularity from 0 to 1. To determine LD volume per cell, thresholded z stacks were subjected to the Volume function of the Slidebook (3i) software.

Data were expressed as means ± SEM. Statistical analysis among groups was performed using Student's t test.

Lipid Extraction and TLC

Fluorescent pulse-chase assays were performed as described earlier, except that 1×10^7 cells were grown in 10-cm dishes and harvested by trypsinization. Lipids were extracted by homogenizing cell pellets in chloroform at 3×10^7 cells per milliliter and then spotted onto silica gel preparative TLC plates (Sigma-Aldrich). Separation of lipids was performed by developing the plates in a solvent system of cyclohexane/ethyl acetate, 1:2 (vol/vol), and fluorescent lipids were visualized using a Typhoon 9410 Molecular Imager (GE Amersham).

Mitochondrial Activity Measurements

Mitochondrial activity was determined using the Seahorse Flux Analyzer XF96, according to the manufacturer's instructions. Briefly, 2×10^4 cells were seeded on 10 μg/ml fibronectin-coated Seahorse 96-well plates. After 24 hr, cells were incubated in CM or HBSS for the time points indicated. Sixteen replicates were performed per cell line, and the average value was taken per experiment. To determine mtOCR, rotenone and antimycin were injected to acutely inhibit mitochondrial-driven oxygen consumption. mtOCR was determined by subtracting nonmitochondrial OCR from total OCR levels. Lipid-oxidation-driven mtOCR was determined by inhibition of the mitochondrial FA importer CPT-I using etomoxir. OCR data were normalized by cell number.

SUPPLEMENTAL INFORMATION

Supplemental Information includes Supplemental Experimental Procedures and seven figures and can be found with this article online at http://dx.doi.org/10.1016/j.devcel.2015.01.029.

AUTHOR CONTRIBUTIONS

A.S.R., S.C., and J.L.-S. designed the research; A.S.R. and S.C. performed research; A.S.R. and S.C. analyzed data; and A.S.R. and J.L.-S. wrote the paper.

ACKNOWLEDGMENTS

We thank N. Mizushima and D.C. Chan for contributing the Atg5KO and Mfn-deficient cell lines, respectively. We thank S. van Engelenburg, T. Lämmermann, and G. Diering for helpful discussions and technical assistance. We are thankful to C. Stratakis for providing access to the Seahorse Flux Analyzer. We thank A. Hoofring for help with illustrations. A.S.R. was supported by a postdoctoral fellowship from the Deutsche Forschungsgemeinschaft.

Received: June 23, 2014
Revised: November 6, 2014
Accepted: January 22, 2015
Published: March 5, 2015

REFERENCES

Axe, E.L., Walker, S.A., Manifava, M., Chandra, P., Roderick, H.L., Habermann, A., Griffiths, G., and Ktistakis, N.T. (2008). Autophagosome formation from membrane compartments enriched in phosphatidylinositol 3-phosphate and dynamically connected to the endoplasmic reticulum. J. Cell Biol. *182*, 685–701.

Bjørkøy, G., Lamark, T., Brech, A., Outzen, H., Perander, M., Overvatn, A., Stenmark, H., and Johansen, T. (2005). p62/SQSTM1 forms protein aggregates degraded by autophagy and has a protective effect on huntingtin-induced cell death. J. Cell Biol. *171*, 603–614.

Cabodevilla, A.G., Sánchez-Caballero, L., Nintou, E., Boiadjieva, V.G., Picatoste, F., Gubern, A., and Claro, E. (2013). Cell survival during complete nutrient deprivation depends on lipid droplet-fueled β-oxidation of fatty acids. J. Biol. Chem. *288*, 27777–27788.

Calder, P.C. (2013). Long chain fatty acids and gene expression in inflammation and immunity. Curr. Opin. Clin. Nutr. Metab. Care *16*, 425–433.

Chen, H., Chomyn, A., and Chan, D.C. (2005). Disruption of fusion results in mitochondrial heterogeneity and dysfunction. J. Biol. Chem. *280*, 26185–26192.

Cogliati, S., Frezza, C., Soriano, M.E., Varanita, T., Quintana-Cabrera, R., Corrado, M., Cipolat, S., Costa, V., Casarin, A., Gomes, L.C., et al. (2013). Mitochondrial cristae shape determines respiratory chain supercomplexes assembly and respiratory efficiency. Cell *155*, 160–171.

Currie, E., Schulze, A., Zechner, R., Walther, T.C., and Farese, R.V., Jr. (2013). Cellular fatty acid metabolism and cancer. Cell Metab. *18*, 153–161.

Dalen, K.T., Dahl, T., Holter, E., Arntsen, B., Londos, C., Sztalryd, C., and Nebb, H.I. (2007). LSDP5 is a PAT protein specifically expressed in fatty acid oxidizing tissues. Biochim. Biophys. Acta *1771*, 210–227.

Dietrich, M.O., Liu, Z.W., and Horvath, T.L. (2013). Mitochondrial dynamics controlled by mitofusins regulate Agrp neuronal activity and diet-induced obesity. Cell *155*, 188–199.

Dupont, N., Chauhan, S., Arko-Mensah, J., Castillo, E.F., Masedunskas, A., Weigert, R., Robenek, H., Proikas-Cezanne, T., and Deretic, V. (2014). Neutral lipid stores and lipase PNPLA5 contribute to autophagosome biogenesis. Curr. Biol. *24*, 609–620.

Eaton, S. (2002). Control of mitochondrial beta-oxidation flux. Prog. Lipid Res. *41*, 197–239.

Eaton, S., Pourfarzam, M., and Bartlett, K. (1996). The effect of respiratory chain impairment of beta-oxidation in rat heart mitochondria. Biochem. J. *319*, 633–640.

Eisner, V., Lenaers, G., and Hajnóczky, G. (2014). Mitochondrial fusion is frequent in skeletal muscle and supports excitation-contraction coupling. J. Cell Biol. *205*, 179–195.

Finn, P.F., and Dice, J.F. (2006). Proteolytic and lipolytic responses to starvation. Nutrition *22*, 830–844.

Frezza, C., Cipolat, S., Martins de Brito, O., Micaroni, M., Beznoussenko, G.V., Rudka, T., Bartoli, D., Polishuck, R.S., Danial, N.N., De Strooper, B., and Scorrano, L. (2006). OPA1 controls apoptotic cristae remodeling independently from mitochondrial fusion. Cell *126*, 177–189.

Fritz, I.B., Davis, D.G., Holtrop, R.H., and Dundee, H. (1958). Fatty acid oxidation by skeletal muscle during rest and activity. Am. J. Physiol. *194*, 379–386.

Furuhashi, M., and Hotamisligil, G.S. (2008). Fatty acid-binding proteins: role in metabolic diseases and potential as drug targets. Nat. Rev. Drug Discov. *7*, 489–503.

Galloway, C.A., and Yoon, Y. (2012). Perspectives on: SGP symposium on mitochondrial physiology and medicine: what comes first, misshape or dysfunction? The view from metabolic excess. J. Gen. Physiol. *139*, 455–463.

Galloway, C.A., and Yoon, Y. (2013). Mitochondrial morphology in metabolic diseases. Antiox. Redox Signal. *19*, 415–430.

Gomes, L.C., Di Benedetto, G., and Scorrano, L. (2011). During autophagy mitochondria elongate, are spared from degradation and sustain cell viability. Nat. Cell Biol. *13*, 589–598.

Granneman, J.G., Moore, H.P., Mottillo, E.P., Zhu, Z., and Zou, L. (2011). Interactions of perilipin-5 (Plin5) with adipose triglyceride lipase. J. Biol. Chem. *286*, 5126–5135.

Grynberg, A., and Demaison, L. (1996). Fatty acid oxidation in the heart. J. Cardiovasc. Pharmacol. *28* (*Suppl 1*), S11–S17.

Haemmerle, G., Moustafa, T., Woelkart, G., Büttner, S., Schmidt, A., van de Weijer, T., Hesselink, M., Jaeger, D., Kienesberger, P.C., Zierler, K., et al. (2011). ATGL-mediated fat catabolism regulates cardiac mitochondrial function via PPAR-α and PGC-1. Nat. Med. *17*, 1076–1085.

Hayashi-Nishino, M., Fujita, N., Noda, T., Yamaguchi, A., Yoshimori, T., and Yamamoto, A. (2009). A subdomain of the endoplasmic reticulum forms a cradle for autophagosome formation. Nat. Cell Biol. *11*, 1433–1437.

Herms, A., Bosch, M., Ariotti, N., Reddy, B.J., Fajardo, A., Fernandez-Vidal, A., Alvarez-Guaita, A., Fernandez-Rojo, M.A., Rentero, C., Tebar, F., et al. (2013). Cell-to-cell heterogeneity in lipid droplets suggests a mechanism to reduce lipotoxicity. Curr. Biol. *23*, 1489–1496.

Hoppins, S., and Nunnari, J. (2009). The molecular mechanism of mitochondrial fusion. Biochim. Biophys. Acta *1793*, 20–26.

Hoppins, S., Lackner, L., and Nunnari, J. (2007). The machines that divide and fuse mitochondria. Annu. Rev. Biochem. *76*, 751–780.

Jägerström, S., Polesie, S., Wickström, Y., Johansson, B.R., Schröder, H.D., Højlund, K., and Boström, P. (2009). Lipid droplets interact with mitochondria using SNAP23. Cell Biol. Int. *33*, 934–940.

Kassan, A., Herms, A., Fernández-Vidal, A., Bosch, M., Schieber, N.L., Reddy, B.J., Fajardo, A., Gelabert-Baldrich, M., Tebar, F., Enrich, C., et al. (2013). Acyl-CoA synthetase 3 promotes lipid droplet biogenesis in ER microdomains. J. Cell Biol. *203*, 985–1001.

Kerner, J., and Hoppel, C. (2000). Fatty acid import into mitochondria. Biochim. Biophys. Acta *1486*, 1–17.

Kim, K.H., Jeong, Y.T., Oh, H., Kim, S.H., Cho, J.M., Kim, Y.N., Kim, S.S., Kim, H., Hur, K.Y., Kim, H.K., et al. (2013). Autophagy deficiency leads to protection from obesity and insulin resistance by inducing Fgf21 as a mitokine. Nat. Med. *19*, 83–92.

Krahmer, N., Farese, R.V., Jr., and Walther, T.C. (2013). Balancing the fat: lipid droplets and human disease. EMBO Mol. Med. *5*, 905–915.

Kristensen, A.R., Schandorff, S., Høyer-Hansen, M., Nielsen, M.O., Jäättelä, M., Dengjel, J., and Andersen, J.S. (2008). Ordered organelle degradation during starvation-induced autophagy. Mol. Cell. Proteomics *7*, 2419–2428.

Mitra, K., Wunder, C., Roysam, B., Lin, G., and Lippincott-Schwartz, J. (2009). A hyperfused mitochondrial state achieved at G1-S regulates cyclin E buildup and entry into S phase. Proc. Natl. Acad. Sci. USA *106*, 11960–11965.

Mizushima, N. (2007). Autophagy: process and function. Genes Dev. *21*, 2861–2873.

Mizushima, N., Yamamoto, A., Hatano, M., Kobayashi, Y., Kabeya, Y., Suzuki, K., Tokuhisa, T., Ohsumi, Y., and Yoshimori, T. (2001). Dissection of autophagosome formation using Apg5-deficient mouse embryonic stem cells. J. Cell Biol. *152*, 657–668.

Nada, M.A., Rhead, W.J., Sprecher, H., Schulz, H., and Roe, C.R. (1995). Evidence for intermediate channeling in mitochondrial beta-oxidation. J. Biol. Chem. *270*, 530–535.

O'Neill, H.M., Holloway, G.P., and Steinberg, G.R. (2013). AMPK regulation of fatty acid metabolism and mitochondrial biogenesis: implications for obesity. Mol. Cell. Endocrinol. *366*, 135–151.

Ouimet, M., Franklin, V., Mak, E., Liao, X., Tabas, I., and Marcel, Y.L. (2011). Autophagy regulates cholesterol efflux from macrophage foam cells via lysosomal acid lipase. Cell Metab. *13*, 655–667.

Peterson, T.R., Sengupta, S.S., Harris, T.E., Carmack, A.E., Kang, S.A., Balderas, E., Guertin, D.A., Madden, K.L., Carpenter, A.E., Finck, B.N., and Sabatini, D.M. (2011). mTOR complex 1 regulates lipin 1 localization to control the SREBP pathway. Cell *146*, 408–420.

Rambold, A.S., Kostelecky, B., Elia, N., and Lippincott-Schwartz, J. (2011). Tubular network formation protects mitochondria from autophagosomal degradation during nutrient starvation. Proc. Natl. Acad. Sci. USA *108*, 10190–10195.

Schaefer, J., Pourfarzam, M., Bartlett, K., Jackson, S., and Turnbull, D.M. (1995). Fatty acid oxidation in peripheral blood cells: characterization and use for the diagnosis of defects of fatty acid oxidation. Pediatr. Res. *37*, 354–360.

Schulze, R.J., Weller, S.G., Schroeder, B., Krueger, E.W., Chi, S., Casey, C.A., and McNiven, M.A. (2013). Lipid droplet breakdown requires dynamin 2 for vesiculation of autolysosomal tubules in hepatocytes. J. Cell Biol. *203*, 315–326.

Shaw, C.S., Jones, D.A., and Wagenmakers, A.J. (2008). Network distribution of mitochondria and lipid droplets in human muscle fibres. Histochem. Cell Biol. *129*, 65–72.

Shibata, M., Yoshimura, K., Furuya, N., Koike, M., Ueno, T., Komatsu, M., Arai, H., Tanaka, K., Kominami, E., and Uchiyama, Y. (2009). The MAP1-LC3 conjugation system is involved in lipid droplet formation. Biochem. Biophys. Res. Commun. *382*, 419–423.

Shibata, M., Yoshimura, K., Tamura, H., Ueno, T., Nishimura, T., Inoue, T., Sasaki, M., Koike, M., Arai, H., Kominami, E., and Uchiyama, Y. (2010). LC3, a microtubule-associated protein1A/B light chain3, is involved in cytoplasmic lipid droplet formation. Biochem. Biophys. Res. Commun. *393*, 274–279.

Singh, R., Kaushik, S., Wang, Y., Xiang, Y., Novak, I., Komatsu, M., Tanaka, K., Cuervo, A.M., and Czaja, M.J. (2009a). Autophagy regulates lipid metabolism. Nature *458*, 1131–1135.

Singh, R., Xiang, Y., Wang, Y., Baikati, K., Cuervo, A.M., Luu, Y.K., Tang, Y., Pessin, J.E., Schwartz, G.J., and Czaja, M.J. (2009b). Autophagy regulates adipose mass and differentiation in mice. J. Clin. Invest. *119*, 3329–3339.

Smirnova, E., Goldberg, E.B., Makarova, K.S., Lin, L., Brown, W.J., and Jackson, C.L. (2006). ATGL has a key role in lipid droplet/adiposome degradation in mammalian cells. EMBO Rep. *7*, 106–113.

Sturmey, R.G., O'Toole, P.J., and Leese, H.J. (2006). Fluorescence resonance energy transfer analysis of mitochondrial:lipid association in the porcine oocyte. Reproduction *132*, 829–837.

Tarnopolsky, M.A., Rennie, C.D., Robertshaw, H.A., Fedak-Tarnopolsky, S.N., Devries, M.C., and Hamadeh, M.J. (2007). Influence of endurance exercise training and sex on intramyocellular lipid and mitochondrial ultrastructure, substrate use, and mitochondrial enzyme activity. Am. J. Physiol. Regul. Integr. Comp. Physiol. *292*, R1271–R1278.

Thumser, A.E., and Storch, J. (2007). Characterization of a BODIPY-labeled fluorescent fatty acid analogue. Binding to fatty acid-binding proteins, intracellular localization, and metabolism. Mol. Cell. Biochem. *299*, 67–73.

Tondera, D., Grandemange, S., Jourdain, A., Karbowski, M., Mattenberger, Y., Herzig, S., Da Cruz, S., Clerc, P., Raschke, I., Merkwirth, C., et al. (2009). SLP-2 is required for stress-induced mitochondrial hyperfusion. EMBO J. *28*, 1589–1600.

Unger, R.H., Clark, G.O., Scherer, P.E., and Orci, L. (2010). Lipid homeostasis, lipotoxicity and the metabolic syndrome. Biochim. Biophys. Acta *1801*, 209–214.

Valetti, C., Wetzel, D.M., Schrader, M., Hasbani, M.J., Gill, S.R., Kreis, T.E., and Schroer, T.A. (1999). Role of dynactin in endocytic traffic: effects of dynamitin overexpression and colocalization with CLIP-170. Mol. Biol. Cell *10*, 4107–4120.

Vock, R., Hoppeler, H., Claassen, H., Wu, D.X., Billeter, R., Weber, J.M., Taylor, C.R., and Weibel, E.R. (1996). Design of the oxygen and substrate pathways. VI. structural basis of intracellular substrate supply to mitochondria in muscle cells. J. Exp. Biol. *199*, 1689–1697.

Wahli, W., and Michalik, L. (2012). PPARs at the crossroads of lipid signaling and inflammation. Trends Endocrinol. Metab. *23*, 351–363.

Walther, T.C., and Farese, R.V., Jr. (2012). Lipid droplets and cellular lipid metabolism. Annu. Rev. Biochem. *81*, 687–714.

Wang, S., Soni, K.G., Semache, M., Casavant, S., Fortier, M., Pan, L., and Mitchell, G.A. (2008). Lipolysis and the integrated physiology of lipid energy metabolism. Mol. Genet. Metab. *95*, 117–126.

Wang, H., Wei, E., Quiroga, A.D., Sun, X., Touret, N., and Lehner, R. (2010). Altered lipid droplet dynamics in hepatocytes lacking triacylglycerol hydrolase expression. Mol. Biol. Cell *21*, 1991–2000.

Wang, H., Sreenivasan, U., Hu, H., Saladino, A., Polster, B.M., Lund, L.M., Gong, D.W., Stanley, W.C., and Sztalryd, C. (2011). Perilipin 5, a lipid droplet-associated protein, provides physical and metabolic linkage to mitochondria. J. Lipid Res. *52*, 2159–2168.

Watmough, N.J., Bhuiyan, A.K., Bartlett, K., Sherratt, H.S., and Turnbull, D.M. (1988). Skeletal muscle mitochondrial beta-oxidation. A study of the products of oxidation of [U-14C]hexadecanoate by h.p.l.c. using continuous on-line radiochemical detection. Biochem. J. *253*, 541–547.

Welte, M.A., Cermelli, S., Griner, J., Viera, A., Guo, Y., Kim, D.H., Gindhart, J.G., and Gross, S.P. (2005). Regulation of lipid-droplet transport by the perilipin homolog LSD2. Curr. Biol. *15*, 1266–1275.

Wolins, N.E., Quaynor, B.K., Skinner, J.R., Tzekov, A., Corce, M.A., Gropler, M.C., Yamaguchi, T., Matsushita, S., Motojima, K., Hirose, F., and Osumi, T. (2006). MLDP, a novel PAT family protein localized to lipid droplets and enriched in the heart, is regulated by peroxisome proliferator-activated receptor alpha. J. Biol. Chem. *281*, 14232–14240.

Yamaguchi, T., Matsushita, S., Motojima, K., Hirose, F., and Osumi, T. (2006). MLDP, a novel PAT family protein localized to lipid droplets and enriched in the heart, is regulated by peroxisome proliferator-activated receptor alpha. J. Biol. Chem. *281*, 14232–14240.

Ylä-Anttila, P., Vihinen, H., Jokitalo, E., and Eskelinen, E.L. (2009). 3D tomography reveals connections between the phagophore and endoplasmic reticulum. Autophagy *5*, 1180–1185.

Yoon, Y., Galloway, C.A., Jhun, B.S., and Yu, T. (2011). Mitochondrial dynamics in diabetes. Antioxid. Redox Signal. *14*, 439–457.

Zechner, R., Zimmermann, R., Eichmann, T.O., Kohlwein, S.D., Haemmerle, G., Lass, A., and Madeo, F. (2012). FAT SIGNALS—lipases and lipolysis in lipid metabolism and signaling. Cell Metab. *15*, 279–291.